Science of the Total Environment 857 (2023) 159409

Contents lists available at ScienceDirect

Science of the Total Environment

journal homepage: www.elsevier.com/locate/scitotenv

Control of trace metal distribution and variability in an interdunal wetland

A. Fernández-Ayuso [a,e], C. Kohfahl [b,*], H. Aguilera [a], M. Rodríguez-Rodríguez [c], F. Ruiz-Bermudo [b], C. Serrano-Hidalgo [d], C. Romero-Álvarez [c]

[a] Instituto Geológico y Minero de España (IGME-CSIC), C/Rios Rosas 23, 28003 Madrid, Spain
[b] Instituto Geológico y Minero de España (IGME-CSIC), Plaza de España, Torre Norte, 41013 Sevilla, Spain
[c] Department of Physical, Chemical and Natural Systems, University Pablo de Olavide, 41013 Seville, Spain
[d] Escuela Técnica Superior de Ingenieros de Minas, Universidad Politécnica de Madrid, C/Ríos Rosas, 21, 28003 Madrid, Spain
[e] Universidad Autonoma de Madrid-Campus de Cantoblanco, C/Francisco Tomás y Valiente, 7, 28049 Madrid, Spain

HIGHLIGHTS

- Increasing trace metal concentrations after elongated dry periods
- Dependence of redox conditions on hydraulic head fluctuations due to gas bubble entrapment
- Atmospheric input source of Cu, Zn, Ni, Sb and Tl

GRAPHICAL ABSTRACT

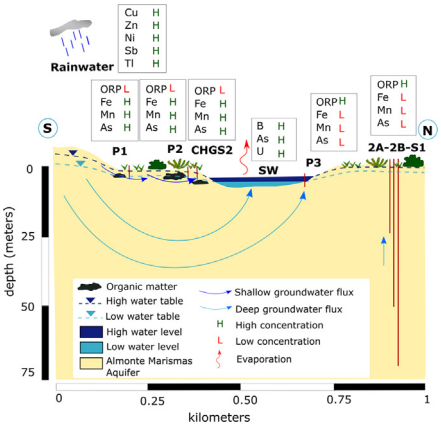

ARTICLE INFO

Editor: José Virgílio Cruz

Keywords:
Trace metal variability
Interdunal wetland
Doñana National Park

ABSTRACT

Trace elements are serious pollutants in the natural environment and are of increasing concern due to the adverse effects at global scale. To refine the current understanding of trace metal distribution and variability in natural environments, concentrations of dissolved trace metals (Ag, Al, As, B, Ba, Be, Co, Cr, Cd, Cu, Fe, Hg, Mo, Ni, Pb, Sb, Se, Th,Tl, U, V, Mn, Zn), major ions, inorganic nutrients (NO_3, PO_4), TOC and stable isotopes of water were determined in water samples from rainwater, seven piezometers and a pond in the coastal Doñana wetland during four sampling campaigns between 2017 and 2019. Results show clear evaporation signatures of stable isotopes in the pond but not in the groundwater. Hydrochemical analyses yield significant, systematic changes in groundwater trace metal and nutrient composition along the flowpath from the dune belt to the pond, controlled by organic matter in the sediments. Whereas major ions reached maximum concentrations in the pond due to evapoconcentration, most trace metals showed highest concentrations at sites with lower redox levels, except for B, As and U, which showed very high concentrations in the pond. Cu, Zn, Ni, Sb and Tl yielded higher median concentrations in rainwater than in most of the groundwater points and in case of Cu and Zn higher even than in surface water which points to an atmospheric input source of these elements. Temporal variability of trace metals was related to lower hydraulic heads after an elongated dry period which led to lower redox levels and higher concentrations of most of the trace elements whereas

* Corresponding author.
E-mail address: c.kohfahl@igme.es (C. Kohfahl).

http://dx.doi.org/10.1016/j.scitotenv.2022.159409
Received 27 June 2022; Received in revised form 4 October 2022; Accepted 9 October 2022
Available online 13 October 2022

major ions showed more constant concentration levels. This is of special concern regarding climate change and the predicted higher frequency of prolonged dry periods, which could modify the natural hydrochemical patterns in undisturbed wetlands systems.

1. Introduction

Trace elements, the so-called heavy metals, are one of the serious pollutants in the natural environment because of their persistence, toxicity, and bioaccumulation and are of increasing environmental concern (Thuong et al., 2013). Over the last decades, global and climate change has drastically modified natural ecosystems and is considered as a major driving force of land degradation in multiple regions (Xiangying et al., 2020). Furthermore, anthropogenic sources of groundwater contaminations, such as industrial and mining wastes as well as the excessive use of chemical products in crop fields, can be the cause of significant changes in the hydrochemistry of an aquifer (Ghobadi et al., 2020).

However, natural processes also control trace metal concentrations in groundwater and surface water. These processes include sorption/desorption, precipitation/dissolution and biological uptake or release. The specific importance of each process for the individual element depends on its soluble form and oxidation state but also on the in-situ parameters pH, oxidation-reduction potential (ORP), surrounding mineral assemblage, organic matter composition and microbial activities. Therefore, and due to the superimposition and interdependence of the different processes, the interpretation of trace metal concentrations and variability under field conditions is extremely complex (Grybos et al., 2007).

Nonetheless, hydrous ferric oxides (HFO) are of critical importance in the sorption of ions onto rocks, soils and sediments. Thus, mobilization and immobilization of potentially toxic elements from geogenic materials are often controlled by redox processes and pH (Mapoma et al., 2016; Hermann and Neumann-Mahlkau, 1985). Redox gradients play a crucial role in controlling the geochemical behavior of elements such as Fe, Mn, V, Cr, and Mo, (O'Connor et al., 2015; Hamer et al., 2020), as well as surface interactions adsorption and precipitation-dissolution (Deverel et al., 2012). Donahoe and Liu (1998) found out that redox processes in the pore water-sediment were responsible for the distribution of many major and trace elements. They also identified the vertical and spatial variation of such elements in a wetland area.

Besides HFO, Natural Organic Matter (NOM), also named humic substances (HS), significantly control the sorption of metal ions onto mineral surfaces in soils and sediments. NOM originates from the degradation of biological material through complex mechanisms and shows a heterogeneous structure which remains poorly characterized (Reiller and Buckau, 2012; Reiller, 2012). Their carboxylate and phenolate functional groups are able to adsorb specific trace metals forming metal-dissolved organic matter (M-DOM) complexes. However, these complexes can also be adsorbed on mineral surfaces and thus immobilize the adsorbed trace metal load (Avena and Koopal, 1998). Since sorption is a charge-dependent process, it highly depends on the pH value of the solution. Neutral or basic pH values may lead to negative charges on both, mineral surfaces and organic matter (OM) leading to dissolved organic matter (DOM) generation and mobilization of trace metals (Grybos et al., 2007). Grybos et al. (2007) studied the trace metals release and its control by organic matter mobility and Fe-oxyhydroxides reduction. They found that organic matter (OM) release played a dominant role for trace metal mobilization.

On the other hand, the key role of vegetation in the water quality of wetlands has also been studied by various authors. Çelebi (2016) and Bonanno et al. (2018), concluded that some plant species have a specific response in terms of translocation and bioindication of trace elements in water and sediments. Bao et al. (2017) studied the pollution of trace metals in a west coastal wetland of the southern Yellow Sea over the last 150 years by means ^{210}Pb and ^{137}Cs dating isotopes, major and trace elements analysis and multivariate statistical methods and clearly illustrates the influence of human activities on the local environment.

Several authors have also studied temporal changes of groundwater hydrochemistry and trace metal concentrations. Thirumala and Kiran (2019) analyzed Fe, Zn, Cu, Pb, Cr, Cd and Mn in groundwater samples of India and found different concentrations comparing pre-monsoon, monsoon and post-monsoon campaigns. Buragohain et al. (2009) analyzed groundwater samples at 20 sites of the Dhemaji district of Assam and found higher trace metal concentrations during the dry seasons. Kuppusamy and Hussain (2021) investigated the seasonal variation for trace metals contamination of groundwater using GIS technology in Goa State, India. Nonetheless, many of these studies are subjected to important time-variant anthropogenic input sources, which hampers the identification of individual natural processes controlling trace metal mobility.

This study enhances current knowledge of trace metal hydrogeochemistry by integrating temporal variations of redox values, major ion chemistry and stable isotope signatures hydrochemistry under almost natural field conditions with very low direct anthropogenic input. The principal objective of this study is to disentangle the different processes of trace metal mobilization under almost natural field conditions. The study is focused (i) on the specific importance of HFO and OM release at different sites for the individual elements and (ii) on the control of temporal or seasonal variability. To meet this objective, determining variables such as in situ parameters, stable isotopes of water, major and minor ion chemistry of ground-, surface- and rainwater were considered.

2. Methods

2.1. Study area

The field site is situated within the Doñana National Park (DNP), which occupies a surface of 543 km^2 in southern Spain (Fig. 1). This area has a sub-humid Mediterranean climate with almost no rainfall in summer and the main precipitation events taking place in autumn and spring. The mean annual precipitation registered in the last 30 years was around 550 mm, most of it during the wet season (October–April). However, interannual variability is not uncommon, and during some years, rainfall concentrates in autumn, while in others it occurs in winter or spring (Naranjo-Fernández et al., 2020).

The DNP is characterized by its great variety of ecosystems. The Park is considered a World Heritage site by UNESCO and is part of the Ramsar Convention. Many of its ecosystems depend on groundwater (Green et al., 2018). The water table depth below the surface ranges from a few centimeters in the discharge sectors to 15 m depth in the dune crests. Besides, the aquifer feeds a large number of ponds, most of them seasonal and some small streams (Fernández-Ayuso et al., 2018).

The uppermost sediments of the DNP are built up by unconsolidated Plio-Quaternary fluvio-marine and alluvial sands, gravels and silts forming the regional Almonte–Marismas aquifer (De Castro and Reinoso, 1997). To the west, they are covered by aeolian sands of a dune belt, whereas in the eastern part they are overlain by estuary sediments of the saltmarshes. The dune belt shows a variable thickness of several meters. Aeolian sands and salt marshes are now forming the major ecosystems of the DNP. The study site is located within the aeolian dune belt which is made up of unconfined aeolian sands containing an irregular presence of organic layers. The system's main source of recharge is direct infiltration from precipitation into the unconfined part of the aquifer. Extractions have increased since the mid-1970s (Olías et al., 2008), threatening groundwater quality and quantity. At a regional scale, groundwater discharges as seepage (i) to the ocean, (ii) to the salt-marshes and (iii) to the many small phreatic wetlands situated on top of the aeolian sands (Manzano et al., 2008).

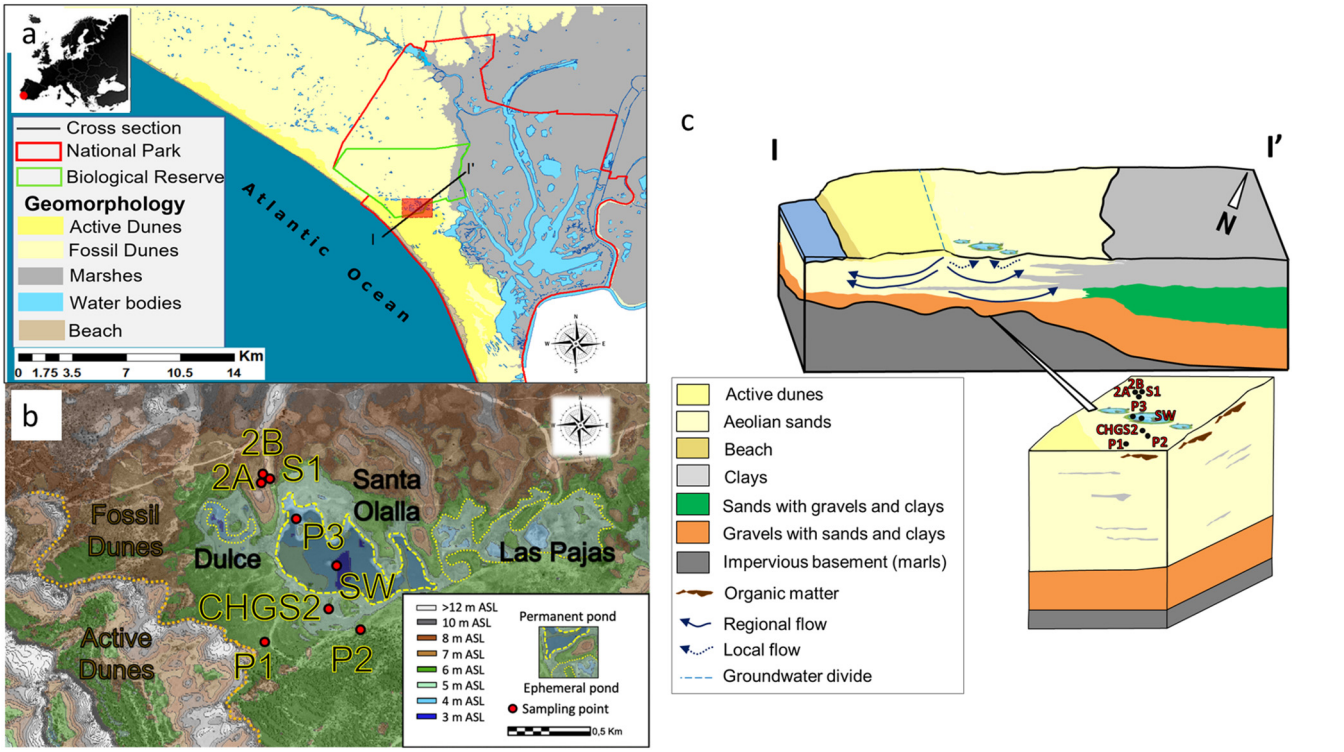

Fig. 1. a) Geology of the Doñana area; b) Enlarged map section of the rectangle in (a) with sampling points and topography (source: Modelo Digital de Terreno Andalucía); c) Sketch of the cross section in the Santa Olalla area. Modified from Serrano-Hidalgo et al. (2021). Dashed lines in b indicate pond limits and the contact between active and fossil dunes.

The hydrochemical groundwater baseline in unconfined areas of the aquifer, at a general scale, is controlled by rainfall composition, which is of Na—Cl facies, equilibrium with silica and dissolution of soil CO_2, Na and K-feldspars and $CaCO_3$ (Manzano et al., 2008). Thus, the mineralization in this aquifer area ranges from very low to moderate.

Despite the numerous works carried out in the DNP, research on hydrochemistry and water quality is scarce and discontinuous over time. These studies were performed at different scales and with different objectives (Olías et al., 2008; Lozano et al., 2001; Manzano et al., 2005, 2008, 2013; Kohfahl et al., 2016). Kohfahl et al. (2016) studied the presence and mobilization of As in groundwater and surface water of the DNP and detected the role of HFO dissolution and competitive sorption as principal processes of As mobilization in ground- and surface water, due to the presence of organic sediments.

The natural composition of the groundwater in areas surrounding the DNP has been modified by agricultural activities nearby, which add to the system a number of pollutants, such as nutrients, metals and/or pesticides. Although the protection of the Doñana area as a National Park has contributed to the conservation of the natural baseline conditions in some parts of the protected area, airborne pollutants coming from a nearby Industrial site, are also cited in the literature (Manzano et al., 2008).

The field site forms a phreatic wetland situated on top of the aeolian sands. It is located directly around the Santa Olalla pond, with a maximum flooded surface of 25 ha forming part of the Dulce-Santa Olalla-Pajas pond system consisting of a semi-permanent (Dulce), permanent (Santa Olalla) and a seasonal pond (Pajas) (Fig. 1). The main groundwater recharge originates from the nearby aeolian dune belt and therefore is assumed not to receive direct anthropogenic impact, e.g., input from creeks or irrigation. The ponds are hydraulically connected and located in depressions of unconfined aeolian sands between stabilized and mobile dunes containing silt and clay lenses at different depths (Sacks et al., 1992). The study site is partly affected by groundwater extraction for human consumption in a nearby tourist resort. Extraction is performed by five pumping wells, some of them located at less than 3.5 km from the investigated sand-dune pond (Fernández-Ayuso et al., 2018).

During years of extremely high rainfall, this system forms one single pond (Díaz-Paniagua et al., 2015). The groundwater flow generally moves from the Northwest to the Southeast and from the southwest dune area towards the Santa Olalla pond (Fig. 2).

2.2. Sampling methods

Sampling points consisted of shallow piezometers (P1, P2, P3 and CHGS2) of less than 5 m depth and additional sampling points of surface water (SW) in the pond (Fig. 2) and rainwater. Three sampling points P1, P2 and CHGS2 were built to sample the hydrochemical evolution along the general groundwater flow path from the dune area towards the pond. In addition, P3 was installed within a temporarily flooded area of the pond to obtain information about groundwater-surface water interaction. To avoid piezometer level alteration by flooding of the pond, the P3 piezometer was constructed from bottom to top with 1 m filter screen, 2 m casing, and a casing top at 1.15 m above surface. Furthermore, deeper water samples have been taken from 3 multilevel piezometers (2A, 2B and S1) located at 190 m distance to P3, at depths between 25 and 30 m (2A), 44 and 46 m (2B) and 67 and 72 m (S1). For isotope analysis, samples from the center (SW_C) and the shore (SW_S) of the Santa Olalla Pond were taken.

The hydraulic heads were monitored with level sensors (OTT-Orpheus Mini in P2, P3, S1, 2A and 2B, and CTD Diver in SW) in an hourly interval. The absolute surface water level was defined as a reference level based on LIDAR (Laser Imaging Detection and Ranging) data from the flight carried out by the National Geographic Institute (IGN) in 2014. The absolute value of hydraulic head at P3 was obtained by in situ measurements of ground- and surface water depth from the piezometer top at P3 during two sampling campaigns under flooding conditions (STable 1, supplementary data). In-situ measurements at P3 revealed a hydraulic head difference of 19 cm

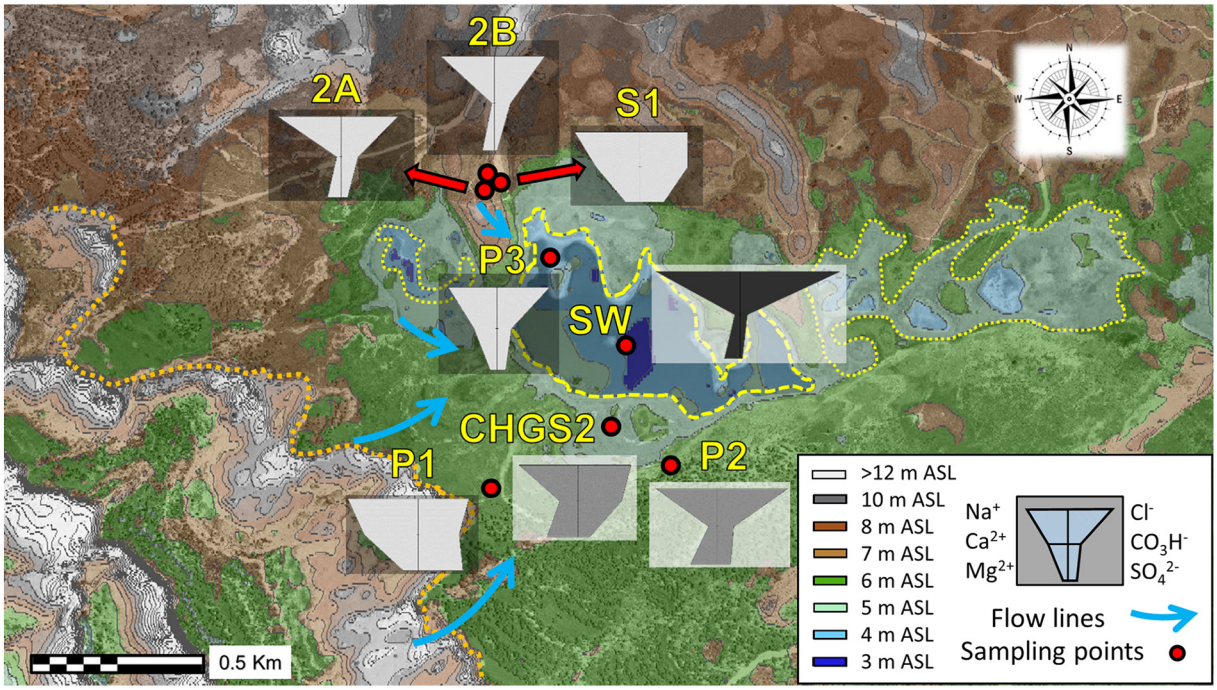

Fig. 2. Groundwater flow direction and Stiff diagram of the water samples taken in May 2019. Light gray sampling points are scaled for a maximum of 3.99 meq/l, 14.20 meq/l for the dark gray points, and 173.46 meq/l for the black diagram representing the surface water sample.

compared to the P3 LIDAR data and therefore the LIDAR time series of P3 was corrected for this value.

Groundwater was sampled from the piezometers by pumping until exchanging two times the water column and after constant values of electrical conductivity and redox potential had been established. Deep water sampling was conducted only on the last date, as it is assumed that, at that depth, no significant temporal changes occur. Groundwater pumps Eijkelkamp and Grundfos were used in the shallow and deep piezometers, respectively. Measurements of pH, temperature, ORP, oxygen and electrical conductivity were carried out in the field in a flow cell, minimizing contact with the atmosphere using HACH HQD meters. Groundwater samples were filtered immediately after sample retrieval through 0.45 μm membrane filters. Alkalinity, NO_2^-, NH_4^+ and Fe^{+2} of filtered samples were determined in the field by titration using Aquamerck colorimetry test kits. Collected samples were stored at 4 °C in polypropylene bottles (50 ml) with watertight caps for subsequent analyses of stable isotopes of water, major and minor ions.

Rainwater was collected in a 5 l high density polyethylene bottle, permanently installed at 4 km distance to the study site. Samples were collected by attaching a funnel to the bottle, which contained paraffin oil to prevent evaporation and the respective accumulated sample volume was registered for each sampling event. Samples were stored without air bubbles in polyethylene bottles of 100 ml volume and conserved immediately at 4 °C in the refrigerator until major and minor ion analysis in the laboratory. Rainwater samples were collected after rainfall periods independently from groundwater sampling, adding up to 13 samples between September 2017 and May 2019.

Four sampling campaigns for ground- and surface water were completed between 2017 and 2019 compiled in Table 1.

Major and minor ion analyses were carried out in the certified IGME-laboratory of the Spanish Geological Survey (CN IGME-CSIC). Sodium (Na^+) and potassium (K^+) analyses were carried out on acidified samples using AES (PTE-AG-007). Anions, calcium (Ca^{2+}) and magnesium (Mg^{2+}) were analyzed by AAS (Varian FS 330). Metals were determined by ICP-MS and total organic carbon (TOC) of groundwater was determined by a total organic carbon analyzer with catalytic oxidation by combustion at 680 °C and detection by NDIR (non-dispersive infrared).

The analyses of the stable isotopes of groundwater and surface water ($\delta^{18}O$ and δ^2H) were carried out at the laboratory of the Center of Hydrogeology of the University of Málaga by using a PICARRO™ L2120-i Cavity Ring-Down Laser Spectrometer. The analytical method consisted of a continuous sequence of three IAEA referred internal standards and seven samples to process the instrumental drifting during the measurement cycles. From each sample, a six injections running-mode was performed, and the first three injections were discarded to avoid memory effects. Blanks for the isotope analyses were analyzed sporadically to confirm there was no memory effect during combustion. The corrected isotope data for $\delta^{18}O$ and δ^2H were reported as 'delta' (δ) values in parts per thousand (denoted as ‰) enrichments or depletions relative to the Vienna-Standard Mean Ocean Water (Rozanski et al., 1993). The accuracy of isotope

Table 1
Sampling campaigns and analyzed parameters of ground- and surface water.

		22/09/2017	07/06/2018	19/10/2018	31/05/2019
	P1	major + minor ions;isotopes,TOC	major + minor ions;isotopes	major + minor ions;isotopes	major + minor ions;isotopes
	P2	major + minor ions;isotopes,TOC	major + minor ions;isotopes	major minor ions;isotopes	major + minor ions;isotopes
	CHGS2	major + minor ions;isotopes,TOC	–	major + minor ions;isotopes	major + minor ions;isotopes
Shallow piezometers	P3	major + minor ions;isotopes,TOC	major + minor ions;isotopes	major + minor ions;isotopes	major + minor ions;isotopes
	2A	–	–	–	major + minor ions;isotopes
	2B	–	–	–	major + minor ions;isotopes
Deep piezometers	S1	–	–	–	major + minor ions;isotopes
Pond	SW	–	major + minor ions;isotopes	major + minor ions;isotopes	major + minor ions;isotopes

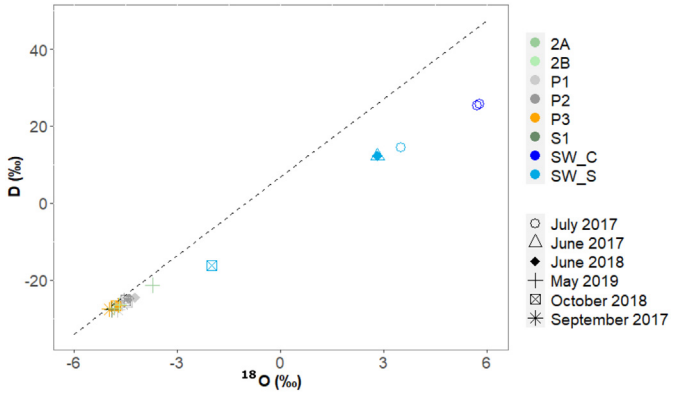

Fig. 3. Isotopes samples from surface water (SW) and groundwater (GW) points. The dotted line corresponds to the LMWL of the years 2014–2018 (Kohfahl et al., 2021). SW_S refers to a sample taken close to the shoreline and SW_C from the center of the pond.

measurements was ±0.1 ‰ for $\delta^{18}O$ and ± 1 ‰ for $\delta^{2}H$. The Local Meteoric Water Line (LMWL) from DNP was estimated from the precipitation weighted least square regression (Kohfahl et al., 2021), within the years 2014–2018, following the equation $\delta^{2}H = 6.8\ \delta 18O + 6.7$.

Rainfall data were collected from the Palacio de Doñana Rain Gauge Station, which belongs to the EBD-CSIC. It is located 4 km from the Santa Olalla Pond. Saturation indexes of the samples were computed using PHREEQC (Parkhurst and Appelo, 2013) with the database LLNL.dat.

To carry out the Principal Component Analysis (PCA) with R software (R Core Team, 2017), the variables were standardized, converting its mean into zero and its standard deviation into 1. Only variables with most data above the detection limit were included. Data below the detection limit, were considered by defining half of value of the detection limit according to usual practice in the PCA analysis. The ORP value of SW in October 2018 used in the PCA (150 mV) is based on Alvarez et al. (2001), since ORP was not measured in this monitoring point during the study period 2017–2019. All the variables included passed the Kaiser-Meyer-Olkin (KMO) factor adequacy test. Graphical results were performed with the R package ggplot2 (Wickham, 2016).

3. Results

3.1. Stable isotopes

Stable isotope analysis of water reveals groundwater samples plotting close to the LMWL, indicating a meteoric source for the groundwater (Fig. 3) discharging into the pond (Kohfahl et al., 2021). Surface water samples show a clear evaporative signature, especially those sampled in the pond's center (SW_C) during the summer months of 2017 and 2018 (Fig. 1). The October sample of 2018 (SW_S) was taken closer to the shoreline, plotting on a mixing line between groundwater and highly evaporated surface water.

3.2. Groundwater types and major ion statistics at the different sites

The spatial distribution of the major ions based on results of the May 2019 sampling campaign is illustrated in Fig. 2. Results show two different

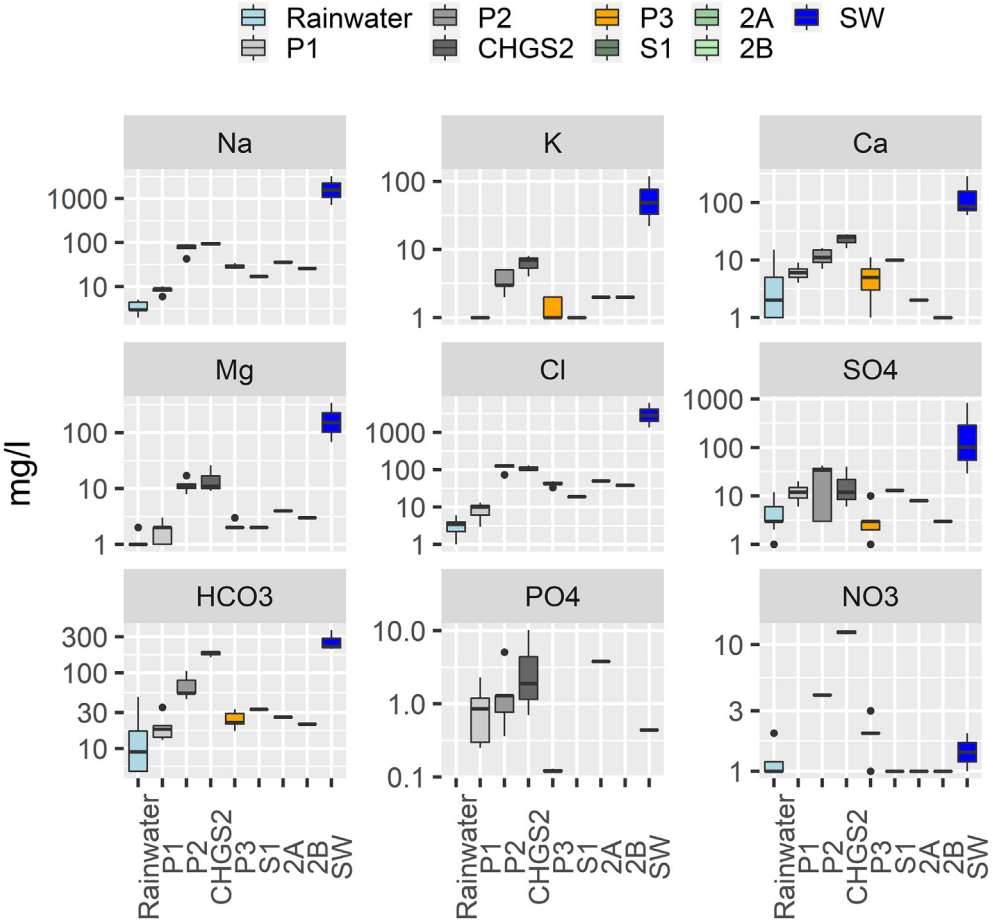

Fig. 4. Boxplot of major ions measured at the sampling points during the four sampling campaigns. For deep piezometers S1, 2A and 2B only one analysis was performed. Concentrations are presented in log scale.

patterns, one group dominated by Na and Cl ions (SW, P2, P3, 2B, 2A) and a second group with higher proportions of Ca, HCO_3 and SO_4 (P1, CHGS2, S1). Moreover, the surface water samples show strong mineralization due to evaporation (STable 1, supplementary data).

The distribution of major ion concentrations at the different sites is shown in Fig. 4.

The boxplots are arranged according to the general flow line from the dune crest to the pond (Fig. 2) starting with rainwater and then following P1, P2, CHGS2, P3 and terminating in the pond (SW). At the deep piezometers S1, 2A and 2B only one analysis was performed but their concentrations were included to enable direct comparison. Except for phosphate and nitrate, results show a general increasing trend along the flow line with maximum concentrations in the pond for most ions, which is attributed to evapoconcentration indicated also by the isotope data shown in Fig. 3. However, the sites P2 and CHGS2 with reducing conditions show local maxima of all components indicating a local and geogenic origin. In contrast, the P3 piezometer, situated directly below the pond (Fig. 2), shows lower mineralization, very similar to those analyzed at the deeper piezometers S1, 2A and 2B. This indicates groundwater discharge of deeper and well oxygenated groundwater into the pond. Nonetheless, all analyzed concentrations of major ions in groundwater remained below the threshold values for human consumption according to the World Health Organization (WHO, 2022).

3.3. In-situ parameters

Parameters measured in situ show low redox potential values (down to −130 mV) for the gray colored shallow piezometers at P1, P2 and CHGS2 (Fig. 5) compared to piezometers P3, S1, 2A and 2B, with oxic conditions.

This is attributed to high amounts of organic carbon detected in sediment analysis of former studies (Kohfahl et al., 2016) and is also in agreement with elevated TOC concentrations especially at P2 and CHGS2 (Fig. 5). This organic material typically accumulates at the front of advancing dune belts where the continued release of drainage water leads to the formation of small local swamps with dense vegetation. In contrast, P3 and deep piezometers (S1, 2A and 2B) located directly beneath the Santa Olalla pond (P3), show positive redox potentials during the complete study period, with higher dissolved oxygen values (STable 1) and low TOC values. Again, the similarity of P3 and the deeper wells indicate a different source origin with a vertical flow path from greater depths without the presence of organic layers. ORP values in surface water measured in former sampling campaigns (Kohfahl et al., 2016) have always shown oxidizing conditions due to the shallow depth below 1 m and its large lateral extension.

3.4. Temporal variability of mayor ions and in-situ parameters

To evaluate temporal changes, the hydraulic heads have been monitored from January 2017 to July 2019, as illustrated in Fig. 6.

Hydraulic heads reflect three major precipitation events with consistent peaks of surface and groundwater levels in the spring of the first two years (2017–2018) and autumn of the last year (2019). Annual oscillations of all piezometers and surface water are within 0.8 m. The deeper piezometers S1

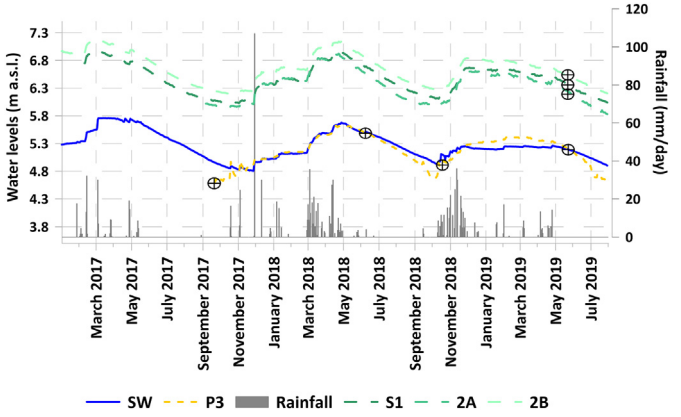

Fig. 6. Daily evolution of rainfall and hydraulic heads during the study period.

2A and 2B show a hydraulic level around 1 m above the shallow piezometers, indicating vertical upward flow and a local discharge to the pond. The hydraulic head between P3 and surface water under flooded conditions shows always equal or higher levels at P3 which is in agreement with hydrochemical data. Periods where the P3 level falls below surface water level were observed only during the dry season where P3 is not flooded and no infiltration may occur.

Nonetheless, the deeper piezometers present an anomaly with a maximum hydraulic head at the intermediate depth of 2B (42 m) and a decreasing head at greater depth S1 (72 m). A possible explanation may be that the deeper S1 is more affected by groundwater extraction of nearby pumping wells at 3.5 km distance, which are screened at 180 m below surface. A similar anomaly was also observed by Fernández-Ayuso et al. (2019) at a nearby multilevel piezometer which is more affected by groundwater extraction.

Results in Fig. 7 show that under suboxic conditions rising water level leads to oxygenation and vice versa, which is visible at points P1, P2 and CHGS2 when comparing low water levels after dry periods in September and October with high water levels in spring after the winter rainfall. This effect is attributed to the uptake of soil gas bubbles by the ascending groundwater level and subsequent oxygen dissolution. The influence of recharge water, rich in oxygen, from the infiltration of rainfall is discarded because it is not reflected by conservative parameters such as Cl.

However, variabilities of most major ions shown in Fig. 8 remain in the same order of magnitude without significant changes. Only phosphate and sulfate show larger variations.

Phosphate shows the highest values at the anoxic sites P2 and CHGS2, which may be related to the often observed release of iron phosphate stored in the sediment by reductive dissolution (Domagalski and Johnson, 2011) which is also in agreement with maximum Fe^{2+} concentrations measured in situ at P2 (Fig. 5). This may explain higher concentrations at P2 and CHGS2 and is further confirmed by the highest values under conditions of lowest redox potentials in September 2017 (STable 1, supplementary data). The low concentrations measured in the Santa Olalla pond are typical for well-oxygenated lake waters because phosphate is usually retained in

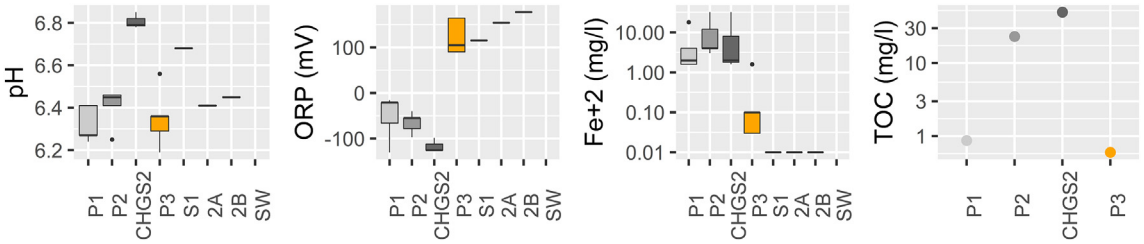

Fig. 5. Box plots of TOC and in-situ parameters (pH, ORP and Fe^{2+}) from the different sampling campaigns. Total organic carbon (TOC) was analyzed in the laboratory at shallow wells on 22.09.2017.

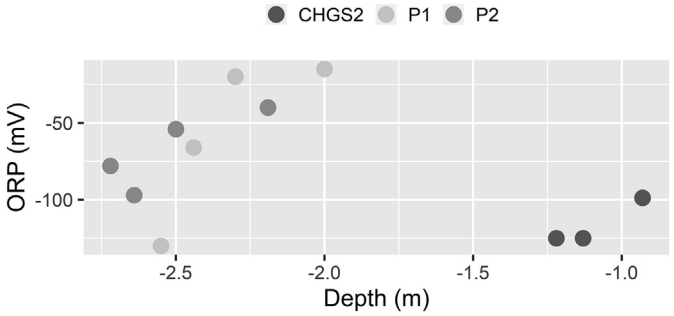

Fig. 7. Scatter plot of depth to hydraulic heads versus redox values at anoxic sites.

the soil by a complex system of biological uptake, absorption, and mineralization (Domagalski and Johnson, 2011).

Also, sulfate concentrations at P2 and CHGS2 show a clear dependence on redox potentials with higher concentrations at less negative values pointing to sulfide oxidation, supported by the respective low Ca/SO_4 ratios in samples with elevated sulfate concentrations (STable 1, supplementary data).

3.5. Spatial variability of minor ions

The box plots of minor ion variability (Fig. 9) show a completely different pattern of spatial variability compared to the major ions.

Except for As, Fe and Mn, which presented elevated concentrations at anoxic sites, the remaining trace metal concentrations were below threshold values for drinking water according to the World Health Organization (WHO, 2022).

Results show different patterns of spatial variability for the individual elements. A first group (B, As, U) shows higher concentrations in the evaporated surface water compared to groundwater. Whereas B and U concentrations in groundwater remained smaller or below detection limit, As also presented elevated concentrations at anoxic groundwater sites.

A second group (Fe, V, Mn, As) showed concentrations several magnitudes higher at anoxic groundwater sites and very low concentrations at the remaining sampling points indicating a strong redox control.

The remaining elements present some intermediate behavior tending to very low concentrations in the surface water and slightly higher concentrations at anoxic sites compared to groundwater sampling points with a higher redox potential.

Cu, Zn, Ni, Sb and Tl yield higher median concentrations in rainwater than in most of the groundwater sites and, in case of Cu and Zn, higher even than in surface water which points to an atmospheric input source of these elements.

3.6. Temporal variability of minor ions

Compared to the major ions, the time series of minor elements show entirely different patterns for many elements (Fig. 10).

Time series show maximum concentrations in the first sampling campaign for a large number of elements which decrease in the second and third campaign (Al, As, Ba, Cr, Fe, Mo, Ni, Th, Tl, V, Zn).

The fact that major ion concentrations do not show these trends and stable isotope data exclude evaporation of groundwater, points to precipitation/dissolution and or sorption/desorption processes triggered by in-situ parameters. As illustrated above, redox values were at their minimum during the first sampling campaign giving rise to dissolution of HFOs with elevated concentrations of Fe and subsequent mobilization of trace metals

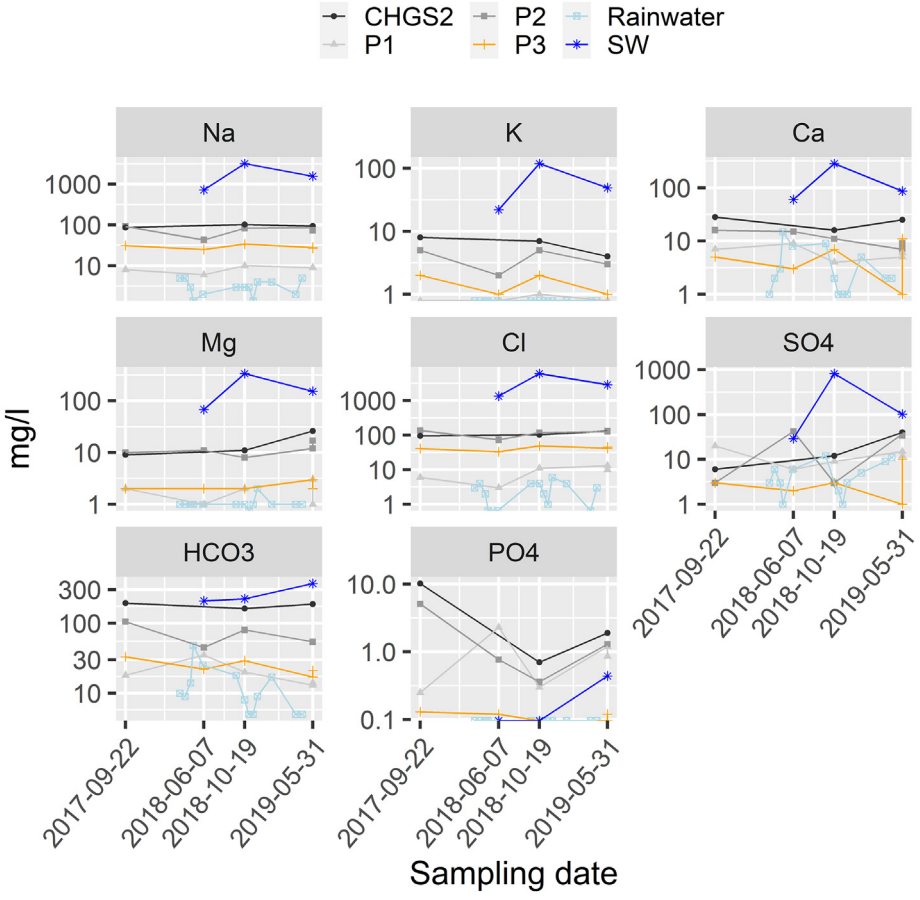

Fig. 8. Time series of major ions at the different sampling sites (concentrations presented in log scale).

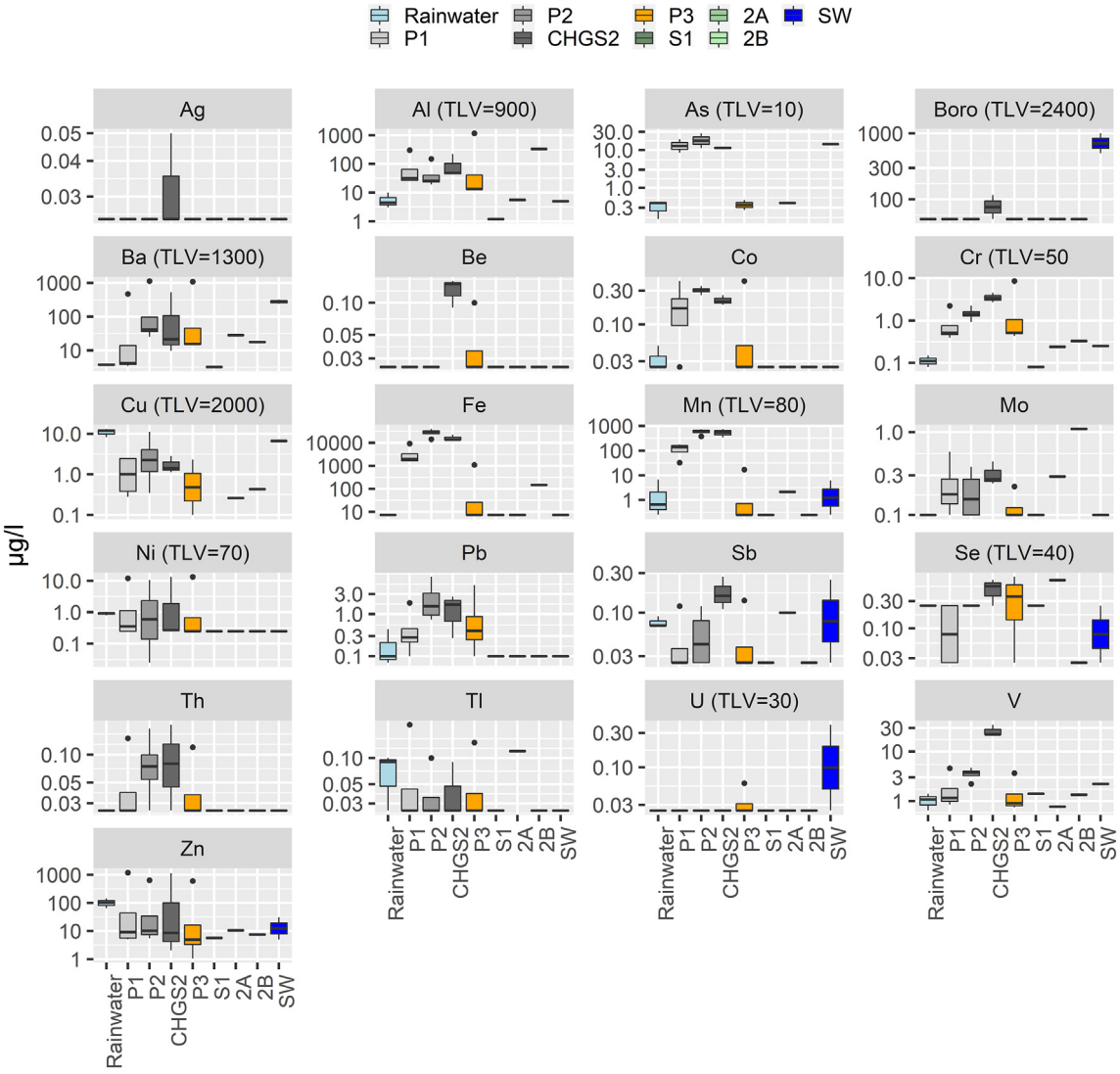

Fig. 9. Boxplot diagram of trace elements grouped by sampling point (µg/L). For deeper piezometers S1, 2A and 2B only one analysis was performed. Cd and Hg were below detection limit in all samples. Concentrations are presented in log scale. Threshold values (TLV) according to WHO (2022) are indicated in µg/l.

(STable 1, supplementary data). In contrast, temporal pH variations at the different groundwater sites were negligible suggesting only a minor influence of OM release on seasonal variability.

3.7. Principal component analysis (PCA)

PCA is a commonly used technique to analyze hydrochemical data. Fig. 11 shows the PCA for the studied sampling points during 2017, 2018 and 2019. PC1 and PC2 are two uncorrelated factors that represent linear combinations of the original variables. In the graph, the length of the arrows represents the variable's variance. The r direction of the arrows points in the direction of increasing values of that variable, and the angle they form between them indicates the correlation between the variables. The smaller the angle (closer to zero) the higher and more positive is the correlation between the variables; the closer the angle to 180°, the more anticorrelated the variables are, and an angle close to 90° indicates the absence of correlation.

Fig. 11 shows that the first component PC1 explains 59 % of the variability and represents the control of the samples by ORP whereas the second component PC2 explains 19 % of the variation. ORP and Fe show the major positive and negative contribution to PC1, respectively. Fe and Mn are highly positive correlated and show strong anticorrelation with ORP because of reductive dissolution of their respective minerals due to their similar behavior under reduced conditions in accordance with the hydrochemical redox-chain. Correlation of Fe with As is related to As mobilization induced by reductive dissolution (Appelo and Postma, 2005).

Al and Zn significantly contribute to the negative part of PC2. They do not change oxidation states under natural conditions and are well correlated among each other but not well correlated with Fe, Mn and As neither with ORP indicating a minor influence of redox conditions. V shows positive correlation with Fe and Mn and negative correlation with ORP whereas Pb shows weaker correlations and represents an intermediate position.

With regard to the sampling locations, Fig. 11 shows 2 endmembers, P3 and CHGS2 representing oxic and reducing conditions respectively, associated with higher metal concentrations under reducing conditions at CHGS2. P1, P2 and SW represent intermediate members between the two previous extremes.

Considering temporal variations, the samples of 2018 and 2019 of the individual sampling points are plotting closely, indicating only minor temporal changes at the respective points within these years. In contrast, samples of 2017 differ from 2018 and 2019. P1, P2 and CHGS2 samples cluster together, showing the lowest values of ORP and higher values of minor ion concentrations, including also V. The 2017 P3 sample also shows higher minor ion concentrations in spite of a high ORP value, which is reflected by a minor influence of PC1 and a higher influence of PC2. The different contribution of principal components in 2017 is reflecting the more

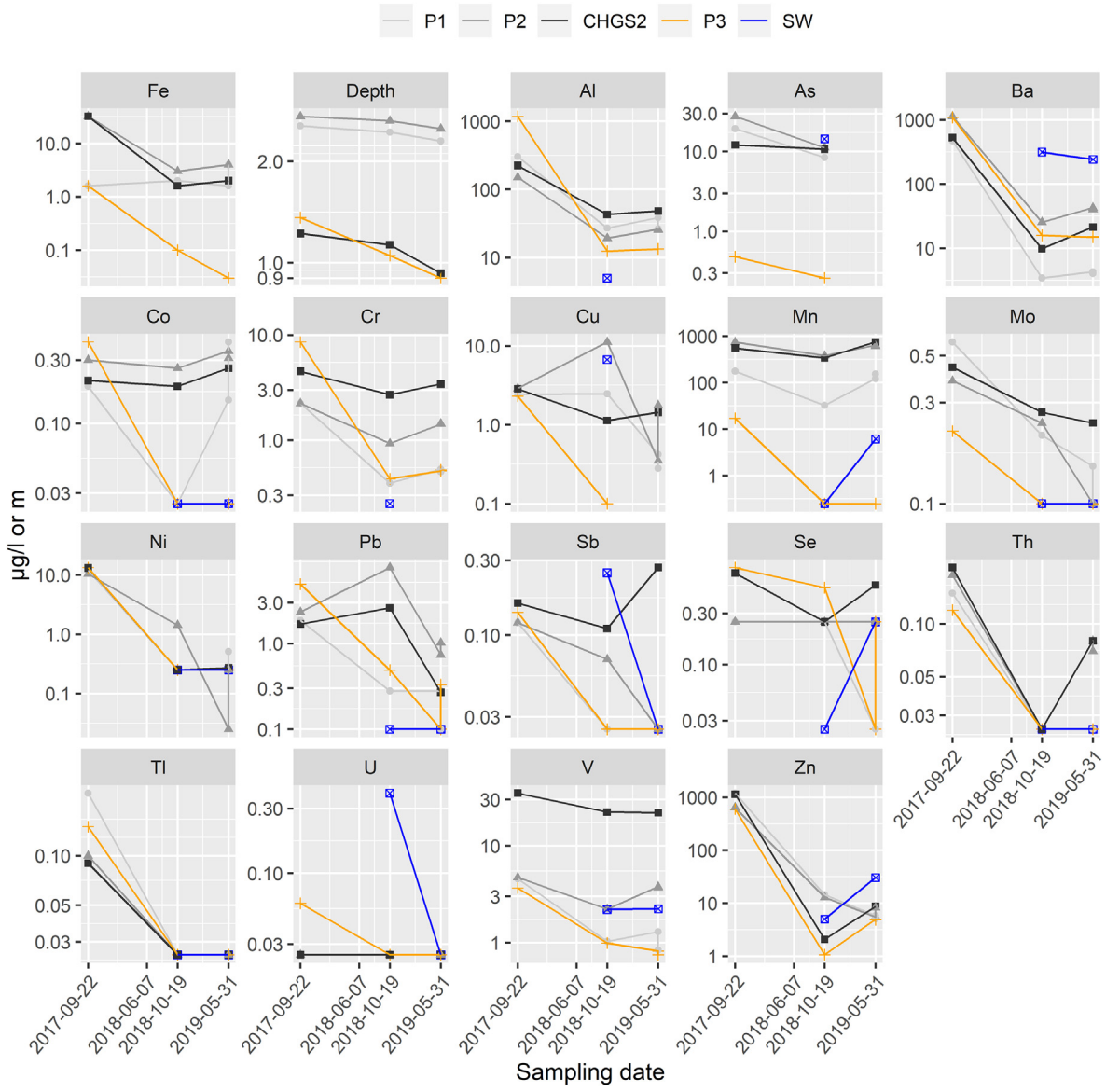

Fig. 10. Time series of minor ions at the shallow piezometers and surface water. Concentrations are given in µg/l, depth refers to depth of hydraulic head from surface given in m. Fe refers to Fe^{2+} analyzed directly in the field. Ag, B and Be were not plotted due to concentrations below detection limit in most of the samples.

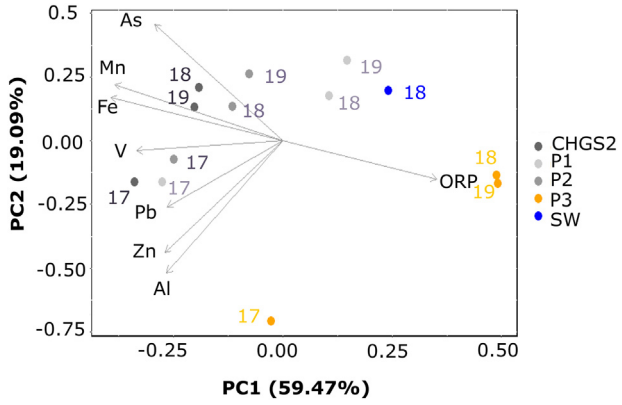

Fig. 11. Principal Component Analysis (PCA) of the trace elements analyzed from the water samples. Numbers refer to the respective years 2017 (17), 2018 (18) and 2019 (19).

elevated minor element concentrations as a result of lower oxygen concentrations after elongated dry periods as discussed above in Fig. 10.

4. Discussion

Based on the analytical results a general evolutionary flow path is proposed for the study area (Fig. 12).

Rainwater infiltrates from the dune crest with sparse vegetation and discharges into the pond. The deeper flow paths do not pass organic layers and show oxic groundwater conditions with lower loads of Fe and Mn (P3, 2A, 2B, S1). In contrast, shallower flow paths are conditioned by organic layers leading to anoxic groundwater with more elevated Fe and Mn concentrations and generally higher trace metal concentrations.

The distribution of trace elements at the different sites described above points to different controls by HFO and OM release. The first group (Fe, Mn, As, V) shows concentrations several magnitudes more elevated at anoxic sites P1, P2 and CHGS2 than at the other sampling points. In the case of Fe, As and Mn, this is attributed to reductive dissolution of HFO under

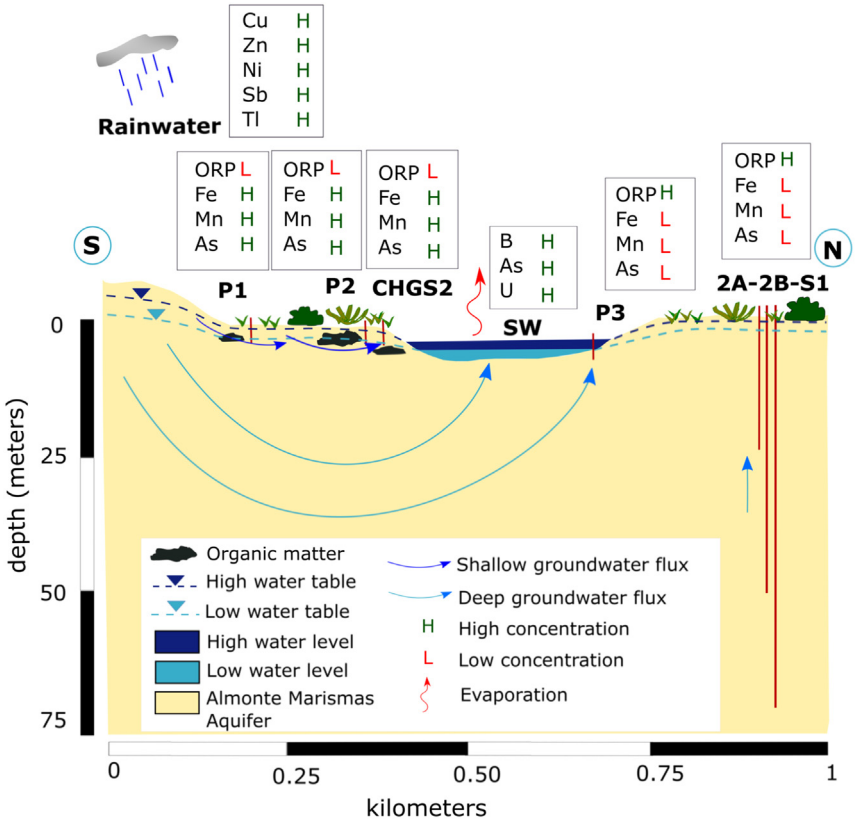

Fig. 12. Hydrogeological sketch showing the main hydrochemical changes along the flow path at the different groundwater sampling sites. The boxes close to their respective sites indicate high (H) and low (L) parameter values measured at the respective sampling point.

reduced conditions. This is in agreement with previous studies and is generally accepted knowledge (Hermann and Neumann-Mahlkau, 1985; Donahoe and Liu, 1998; Yang et al., 2015). Nevertheless, according to Gustafsson (2019), V III is also frequent in reducing environments, but due to the formation of complexes with organic matter instead of reductive HFO dissolution.

Significantly higher concentrations of trace elements in surface water were detected for B and As. PHREEQC simulations yielded uncharged B $(OH)_3$ as dominant species in ground- and surface water and undersaturation of B_2O_3. Therefore, elevated concentrations are attributed to minor influence of sorption and precipitation combined with evapoconcentration. Due to the low groundwater concentrations and the location in a protected remote area, possible wastewater and fertilizer inputs are discarded and the origin is supposed to be geogenic. Natural B inputs are generally related to sea salt sources since B concentrations in rainfall decline with increasing distances from the coast (Jahiruddin et al., 1998). High As concentrations in surface water are related to desorption from HFO surfaces due to competitive sorption with inorganic carbon species related to high alkalinity and elevated pH which was also detected in former studies in the study area by Kohfahl et al. (2016).

The remaining elements presented only slightly higher concentrations at anoxic sites than in oxic groundwater and showed much lower concentrations in the surface water of the pond. This may have different reasons related to the variation of species distribution, mineral solubility and/or OM type at the different sites. For example, the decrease of Al concentrations from oxic groundwater (P3) to surface water is attributed to a solubility decrease due to a pH increase in the pond water confirmed by PHREEQC simulation which yielded oversaturation in Dawsonite ($NaAlCO_3(OH)_2$) for surface water but undersaturation in groundwater (P3). A detailed discussion of all the other remaining elements goes beyond the scope of this article.

High concentrations of Ni, Cu and Zn in rainwater are in agreement with Castillo et al. (2013a), who found that the trace metal load of rainwater in the Doñana area is related to the Huelva industrial pole, located 47 km away from the Santa Olalla pond. A further source may be related to open-pit mines of the Iberian Pyrite Belt, which crop out to the N and NW of Doñana. The predominant winds NW-SE (Castillo et al., 2013b), support this origin of these metals.

The seasonal control of trace metal concentration due to groundwater table fluctuations and subsequent change of redox conditions has been observed also by other authors (Stuyfzand, 1999), albeit in a different context. Following a water-table rise, entrapped bubbles may be dissolved due to the increased hydrostatic pressure and therefore constitute a relevant source of dissolved gases in groundwater (Fry et al., 1997; Mayer et al., 2002; Holojer et al., 2003, Mächler et al., 2013). Though several studies have been carried out dealing with bubble mediated gas transfer into groundwater, little attention has been drawn to the contribution of other potential oxygen pathways. To our knowledge, no study has focused on oxygen pathways and trace metal variability due to natural groundwater oscillations in natural environments so far. This behavior is of special concern regarding climate change and the predicted higher frequency of dry periods, which could eventually increase the metals' content potentially dangerous for the biota (Pradit et al., 2016).

Although the PCA analysis reveals strong anticorrelation of ORP only with Fe, Mn and As, ORP also influenced other less correlated elements such as V. Zn - ORP does not show a significant relation in the PCA analyses but adsorption on iron oxides has been reported by other authors (e.g. Trivedi et al., 2001).

5. Conclusions

The following conclusions can be drawn from this research:

✓ Fe, Mn, As and V are controlled by redox conditions. Whereas elevated Fe, As and Mn concentrations are attributed to reductive HFO dissolution, variability of V may be controlled by OM release.

- ✓ Significantly elevated concentrations of trace elements in surface water were detected only for B, As and U. High As concentrations may be related to desorption of HFO surfaces due to increasing pH and alkalinity in the pond water. PHREEQC simulations yielded uncharged $B(OH)_3$ as dominant species in ground- and surface water and undersaturation of B_2O_3. Therefore, elevated concentrations are attributed to absence of sorption and precipitation combined with evapoconcentration.
- ✓ Due to sorption and mineral precipitation, trace metal concentrations in the pond for the remaining elements are very low or below detection limit.
- ✓ Seasonal hydraulic head fluctuations control redox levels and trace metal concentrations. Rising groundwater increases redox values and decreases trace metal concentrations whereas prolonged dry periods with low hydraulic heads lead to higher trace metal concentrations which may be relevant for climate change scenarios.
- ✓ Cu, Zn, Ni, Sb and Tl yield higher median concentrations in rainwater than in groundwater indicating an atmospheric input source of these elements.

Supplementary data to this article can be found online at https://doi.org/10.1016/j.scitotenv.2022.159409.

CRediT authorship contribution statement

Fernández-Ayuso, A.: Writing, reviewing and editing, figure preparation.

Claus Kohfahl: Funding acquisition, Investigation, Interpretation, Data curation, Project administration, Conceptualization, Methodology, Data processing, figure preparation, writing, reviewing and editing.

Aguilera, H.: Performance and supervision of principal component analysis. Writing, reviewing and editing.

Rodríguez-Rodríguez, M.: Figure preparation, reviewing and editing.

Ruiz-Bermudo, F.: Figure preparation, reviewing and editing.

Serrano-Hidalgo, C.: Figure preparation, reviewing and editing.

Romero-Álvarez, C.: Investigation, interpretation, Figure preparation.

Data availability

Data will be made available on request.

Declaration of competing interest

The authors declare that they have no known competing financial interests or personal relationships that could have appeared to influence the work reported in this paper.

Acknowledgements

This work has been financed by the CLIGRO Project (MICINN, CGL2016-77473-C3-1-R) of the Spanish National Plan for Scientific and Technical Research and Innovation. The infrastructure has been co-financed by European Research Funds (SE Scientific Infrastructures and Techniques and Equipment 388 2013, IGME13-1E-2113). We are especially grateful for the technical support of Lidia Molano Leno and Daniel Jesus Martinez Suárez. The contracts of Lidia Molano Leno (PEJ-2014-A-68763) and Daniel Jesus Martinez Suárez (PTA2014-09579-I) were financed by the Ministry of Economy, Industry and Competitiveness of Spain (MINECO) and co-financed by the European Investment Bank (EIB) and the European Social Fund (ESF). The contract of Carmen Serrano Hidalgo was funded by the Industrial PhD grant supported by the Autonomous Region of Madrid, Spain (IND2018/AMB-9553). This work is also a contribution to the Andalusian research groups RNM-308 (Group of Hydrogeology) and RNM-126 (Group of water resources), the Lower Guadalquivir Basin convention between the CN IGME CSIC and Confederación Hidrológica del Guadalquivir (CHG) as well as the convention between Pablo de Olavide University and the Guadalquivir River Basin Board (Hydrological monitoring and modeling in Doñana temporary ponds).

References

Alvarez, S., Rico, E., Guerrero, M.C., Montes, C., 2001. Decomposition of Juncus maritimus in two shallow lakes of Doñana National Park. Int. Rev. Hydrobiol. 86 (4–5), 541–554.

Appelo, C.A.J., Postma, D., 2005. . URLIn: Appelo, C.A.J., Postma, D. (Eds.), Geochemistry, Groundwater and Pollution, 2nd ed. CRC Press https://doi.org/10.1201/9781439833544.

Avena, M.J., Koopal, L.K., 1998. Desorption of humic acids from an iron oxide surface. Environ. Sci. Technol. 32 (17), 2572–2577.

Bao, K., Shen, J., Sapkota, A., 2017. High-resolution enrichment of trace metals in a west coastal wetland of the southern Yellow Sea over the last 150 years. J. Geochem. Explor. 176, 136–145.

Bonanno, G., Vymazal, J., Cirelli, G.L., 2018. Translocation, accumulation and bioindication of trace elements in wetland plants. Sci. Total Environ. 631, 252–261.

Buragohain, M., Bhuyan, B., Sarma, H.P., 2009. Seasonal distribution of trace metals in groundwater of Dhemaji District, Assam, India. Int.J.Chem.Technol.Res. 1 (4), 1014–1021.

Castillo, S., Jesús, D., de la Campa, A.M.S., González-Castanedo, Y., Fernández-Camacho, R., 2013a. Heavy metal deposition fluxes affecting an Atlantic coastal area in the southwest of Spain. Atmos. Environ. 77, 509–517.

Castillo, S., Jesús, D., de la Campa, A.M.S., González-Castanedo, Y., Fernández-Caliani, J.C., Gonzalez, I., Romero, A., 2013b. Contribution of mine wastes to atmospheric metal deposition in the surrounding area of an abandoned heavily polluted mining district (Rio Tinto mines, Spain). Sci. Total Environ. 449, 363–372.

Çelebi, A., 2016. Trace metal surface water inflow and retention in different terms of the wetland. Desalin. Water Treat. 57 (40), 18806–18816.

World Health Organization, W.H.O.collab, 2022. Guidelines for Drinking-water Quality. Fourth edition. incorporating the first and second Addendum.

De Castro, F., Reinoso, J.M., 1997. Model of long-term water-table dynamics at Doñana National Park. Water Res. 31 (10), 2586–2596.

Deverel, S.J., Goldberg, S., Fujii, R., 2012. Chemistry of trace elements in soils and ground water. In: Wallender, W.W., Tanji, K.K. (Eds.), ASCE Manual and Reports on Engineering Practice no 71. Agricultural Salinity Assessment and Management, 2nd edition, pp. 89–137 Reston VA. Chapter 4.

Díaz-Paniagua, C., Fernández-Zamudio, R., Serrano, L., Florencio, M., Gómez-Rodríguez, C., Sousa, A., Sánchez-Castillo, P., García-Murillo, P., Siljestrom, P., 2015. El Sistema de Lagunas Temporales de Doñana, una Red de Hábitats Acuáticos Singulares. Ed: Naturaleza y Parques Nacionales, Serie Técnica.

Domagalski, J.L., Johnson, H.M., 2011. Comparative study of phosphorus transport in the unsaturated zone, groundwater, streams, and tile drains at five agricultural watersheds, U. S. A. J. Hydrol. 409, 157–171.

Donahoe, R.J., Liu, C., 1998. Pore water geochemistry near the sediment-water interface of a zoned, freshwater wetland in the southeastern United States. Environ. Geol. 33 (2), 143–153.

Fernández-Ayuso, A., Rodríguez-Rodríguez, M., Benavente, J., 2018. Assessment of the hydrological status of Doñana dune ponds: a natural world heritage site under threat. Hydrol. Sci. J. 63 (15–16), 2048–2059.

Fernández-Ayuso, A., Aguilera, H., Guardiola-Albert, C., Rodríguez-Rodríguez, M., Heredia, J., Naranjo-Fernández, N., 2019. Unraveling the hydrological behavior of a coastal pond in Doñana National Park (Southwest Spain). Groundwater 57 (6), 895–906.

Fry, V.A., Selker, J.S., Gorelik, S.M., 1997. Experimental investigations for trapping oxygen gas in saturated porous media. Water Resour. Res. 33, 2687.

Ghobadi, A., Cheraghi, M., Sobhanardakani, S., Lorestani, B., Merrikhpour, H., 2020. Hydrogeochemical characteristics, temporal, and spatial variations for evaluation of groundwater quality of hamedan-bahar plain as a major agricultural region,West of Iran. Environ. Earth Sci. 79 (18), 1–16.

Green, A.J., Bustamante, J., Janss, G.F.E., Fernández-Zamudio, R., Díaz-Paniagua, C., 2018. Doñana Wetlands (Spain). In: Finlayson, C.M., Milton, G.R., Prentice, R.C., N.C.D. (Eds.), The Wetland Book: II: Distribution, Description and Conservation. Springer Netherlands, Dordrecht, pp. 1123–1136 https://doi.org/10.1007/978-94-007-4001-3_139.

Grybos, M., Davranche, M., Gruau, G., Petitjean, P., 2007. Is trace metal release in wetland soils controlled by organic matter mobility or Fe-oxyhydroxides reduction? J. Colloid Interface Sci. 314 (2), 490–501.

Gustafsson, J.P., 2019. Vanadium geochemistry in the biogeosphere –speciation, solid-solution interactions, and ecotoxicity. Appl. Geochem. (ISSN: 0883-2927) 102, 1–25 2019.

Hamer, K., Gudenschwager, I., Pichler, T., 2020. Manganese (Mn) concentrations and the Mn-Fe relationship in shallow groundwater: implications for groundwater monitoring. Soil Syst. 4 (3), 49.

Hermann, R., Neumann-Mahlkau, P., 1985. The mobility of zinc, cadmium, copper, lead, iron and arsenic in ground water as a function of redox potential and pH. Sci. Total Environ. 43 (1–2), 1–12.

Holojer, J., Peeters, F., Aeschbach-Hertig, W., Kinzelbach, W., Kipfer, R., 2003. Kinetic model of gas bubble dissolution in groundwater and its implications for the dissolved gas composition. Environ.Sci. Technol. 37, 1337–1343.

Jahiruddin, M., Smart, R., Wade, A.J., Neal, C., Cresser, M.S., 1998. Factors regulating the distribution of boron in water in the River Dee catchment in north east Scotland. Sci. Total Environ. 210–211, 53–62.

Kohfahl, C., Navarro, D.S.R., Mendoza, J.A., Vadillo, I., Giménez-Forcada, E., 2016. Algae metabolism and organic carbon in sediments determining arsenic mobilisation in ground- and surface water. A field study in Doñana National ParkSpain. Sci. Total Environ. 544, 874–882.

Kohfahl, C., Fonseca Rodríguez, R., Ruiz Bermudo, F., Vadillo, I., 2021. Vapour source and spatiotemporal variation of precipitation isotopes in Southwest Spain. Hydrol. Process. 35 (12), e14445.

Kuppusamy, E., Hussain, S.M., 2021. Seasonal variation for trace metals contamination of groundwater using GIS technology in Pissurlem, Sonshi, Cudnem, Velguem, Surla Watersheds, North Goa District, Goa State, India. Water Resources in Arid Lands: Management and Sustainability. Advances in Science, Technology & Innovation. Springer, Cham https://doi.org/10.1007/978-3-030-67028-3_4.

Lozano, E., Delgado, F., Manzano, M., Custodio, E., 2001. Interacción entre las lagunas freáticas de Doñana (SO España) y el acuífero según los isótopos ambientales. In: Medina, Carrera (Eds.), Las Caras del Agua Subterránea. Congreso en Memoria de Germán Galarza, Barcelona, pp. 379–385.

Mächler, L., Peter, S., Brennwald, M.S., Kipfer, R., 2013. Excess air formation as a mechanism for delivering oxygen to groundwater. Water Resour. Res. 49 (10), 6847–6856.

Manzano, M., Custodio, E., Colomines, M., 2005. El fondo hidroquímico natural del acuífero de Doñana (SO ESPAÑA). Congreso Ibérico de Geoquímica (5°: 2005: Soria). V Congreso Ibérico de Geoquímica y IX Congreso de Geoquímica de España. 2005. Diputación Provincial, Soria 1-13p.

Manzano, M., Custodio, E., Iglesias, M., Lozano, E., 2008. Groundwater baseline composition and geochemical controls in the Doñana aquifer system (SW Spain). In: Edmunds, W.M., Shand, P. (Eds.), Natural Groundwater Quality. Blackwell, pp. 216–232.

Manzano, M., Custodio, E., Lozano, E., Higueras, H., 2013. Relationships between wetlands and the Doñana coastal aquifer (SW Spain). Groundw. Ecosyst. 169, 169–182.

Mapoma, H.W.T., Xie, X., Zhu, Y., Liu, Y., Sitolo-Banda, G.C., 2016. Trace element geochemical evolution and groundwater origin in North Rukuru-Songwe alluvial aquifer of northern Malawi. Environ. Earth Sci. 75 (10), 877.

Mayer, K.U., Frind, E.O., Blowes, D.W., 2002. Multicomponent reactive transport modeling in variably saturated porous media using a generalized formulation for kinetically controlled reactions. Water Resour. Res. 38 (9), 1174–1195.

Naranjo-Fernández, N., Guardiola-Albert, C., Aguilera, H., Serrano-Hidalgo, C., Rodríguez-Rodríguez, M., Fernández-Ayuso, A., Ruiz-Bermudo, F., Montero-González, E., 2020. Relevance of spatio-temporal rainfall variability regarding groundwater management challenges under global change: Case study in Doñana (SW Spain). Stoch. Env. Res. Risk A. 34 (9), 1289–1311.

O'Connor, A.E., Luek, J.L., McIntosh, H., Beck, A.J., 2015. Geochemistry of redox-sensitive trace elements in a shallow subterranean estuary. Mar. Chem. 172, 70–81.

Olías, M., González, F., Cerón, J.C., Bolivar, J.P., González-Labajo, J., García-López, S., 2008. Water qualitiy and distribution of trace elements in the Doñana aquifer (SW spain). Environ. Geol. 55 (7), 1555–1568.

Parkhurst, D.L., Appelo, C.A.J., 2013. Description of Input and Examples for PHREEQC Version 3: A Computer Program for Speciation, Batch-reaction, One-dimensional Transport, and Inverse Geochemical Calculations (No. 6-A43). US Geological Survey.

Pradit, S., Shazili, N.A.M., Towatana, P., Saengmanee, W., 2016. Accumulation of trace metals in Anadara granosa and Anadara inaequivalvis from Pattani Bay and the Setiu Wetlands. Bull. Environ. Contam. Toxicol. 96 (4), 472–477.

R Core Team, 2017. R: a language and environment for statistical computing. URLR Foundation for Statistical Computing, Vienna, Austria. https://www.R-project.org/.

Reiller, P., 2012. Modelling metal–humic substances–surface systems: reasons for success, failure and possible routes for peace of mind. Mineral. Mag. 76 (7), 2643–2658. https://doi.org/10.1180/minmag.2012.076.7.02.

Reiller, P.E., Buckau, G., 2012. Impacts of humic substances on the geochemical behaviour of radionuclides. In: Poinssot, C., Geckeis, H. (Eds.), Radionuclide Behaviour in the Natural Environment: Science, Implications and Lessons for the Nuclear Industry. Woodhead Publishing, Cambridge, UK.

Rozanski, K., Araguás-Araguás, L., Gonfiantini, R., 1993. Isotopic patterns in modern global precipitation. Geophysical Monograph-American Geophysical Union. 78, p. 1.

Sacks, L.A., Herman, J.S., Konikow, L.F., Vela, A.L., 1992. Seasonal dynamics of groundwater-lake interactions at Doñana National ParkSpain. J. Hydrol. 136 (1–4), 123–154.

Serrano-Hidalgo, C., Guardiola-Albert, C., Heredia, J., Elorza Tenreiro, F.J., Naranjo-Fernández, N., 2021. Selecting suitable MODFLOW packages to model pond-groundwater relations using a regional model. Water 13 (8), 1111.

Stuyfzand, P.J., 1999. Patterns in groundwater chemistry resulting from groundwater flow. Hydrogeol. J. 7 (1), 15–27.

Thirumala, S., Kiran, B.R., 2019. Seasonal variations of trace metals in the groundwater samples of Harihara Taluk, Davangere District, Karnataka. Rasayan J. Chem. 12 (3), 1195–1202.

Thuong, N.T., Yoneda, M., Ikegami, M., Takakura, M., 2013. Source discrimination of heavy metals in sediment and water of Lich River in Hanoi City using multivariate statistical approaches. Environ. Monit. Assess. 185 (10), 8065–8075.

Trivedi, P., Axe, L., Tyson, T.A., 2001. An analysis of zinc sorption to amorphous versus crystalline iron oxides using XAS. J. Colloid Interface Sci. (ISSN: 0021-9797) 244 (2), 230–238. https://doi.org/10.1006/jcis.2001.7971 2001.

Wickham, H., 2016. ggplot2: Elegant Graphics for Data Analysis. Springer-Verlag, New York 978-3-319-24277-4.

Xiangying, L., Ding, Y., Han, T., Sillanpää, M., Jing, Z., You, X., Li, G., 2020. Seasonal and interannual changes of river chemistry in the source region of Yellow River, Tibetan Plateau. Appl. Geochem. 119, 104638.

Yang, C., Li, S., Liu, R., Sun, P., Liu, K., 2015. Effect of reductive dissolution of iron (hydr)oxides on arsenic behavior in a water–sediment system: first release, then adsorption. Ecol. Eng. 83, 176–183. https://doi.org/10.1016/j.ecoleng.2015.06.018.